

# Impact of Connection Admission Process on the Direct Retry Load Balancing Algorithm in Cellular Networks

Shaunak Joshi, Przemysław Pawełczak, Sateesh Addepalli, John Villaseñor, and Danijela Čabrić

## Abstract

We present an analytical framework for modeling a priority-based load balancing scheme in cellular networks based on a new algorithm called direct retry with truncated offloading channel resource pool ( $DR_K$ ). The model differs in many respects from previous works on load balancing. Foremost, it incorporates the call admission process, through random access. In specific, the proposed model implements the Physical Random Access Channel used in 3GPP network standards. Furthermore, the proposed model allows the differentiation of users based on their priorities. The quantitative results illustrate that, for example, cellular network operators can control the manner in which traffic is offloaded between neighboring cells by simply manipulating the length of the random access phase. Our analysis allow to quantitatively determine the blocking probability individual users will experience given a specific length of random access phase. Furthermore, we observe that the improvement in blocking probability per shared channel for load balanced users using  $DR_K$  is maximized at an intermediate number of shared channels, as opposed to the maximum number of these shared resources. This occurs because a balance is achieved between the number of users requesting connections and those that are already admitted to the network.

Shaunak Joshi, Przemysław Pawełczak, John Villaseñor, and Danijela Čabrić are with the Department of Electrical Engineering, University of California, Los Angeles, 56-125B Engineering IV Building, Los Angeles, CA 90095-1594, USA (email: {sjoshi, przemek, villa, danijela}@ee.ucla.edu).

Sateesh Addepalli is with Cisco Systems, Inc. San Jose, CA 95134, USA (email: sateeshk@cisco.com).

Part of this work has been accepted to the proceedings of IEEE GLOBECOM, 6-10 Dec., 2010, Miami, FL, USA [1].

## I. INTRODUCTION

Given the rapid current and expected growth in HSPA and LTE-based networks and in the number of mobile devices that use such networks to download data-intensive, multimedia-rich content, the need for QoS-enabled connection management is vital. However, the non-uniform distribution of users and consequent imbalance in usage of radio resources leads to an existence of local areas of under- and over-utilization of these resources in the network. This phenomenon results in challenging network management issues. Load balancing is an important technique that attempts to solve such issues, and occurs when a centralized network controller intelligently distributes connections from highly congested cells to neighboring cells which are less occupied. This allows for an increase in network subscriber satisfaction, as more subscribers meet their QoS requirements. Furthermore, it allows for an increase in overall channel utilization.

Load balancing is popular among the academic community and has been explored for many years as described, for example, in earlier works such as [2], [3], as well as more recently in [4]–[7], and many other papers. For simplicity, in the previous treatment of load balancing, it has been assumed that the connection admission process can be neglected. In cellular networks, however, each new connection needs to first send a request to the serving base station (BS) through some predefined control channel. In 3GPP standards, this control channel is the Physical Random Access Channel [8, Sec. 2.4.4.4], [9, Sec. II]. The success of a connection request by a user is dependent on multiple factors including the number of requesting users; the pairwise channel quality between the user and the serving base station (measured, for example, in BER or outage probability); and the actual control channel access technique itself [10]–[12]. Until now the impact of random access overhead on load balancing performance is not well understood. More specifically, the quantitative relationship between the random access phase length and the user blocking probability in a load balancing-enabled cellular system is unknown.

The present paper aims to provide a framework to address this gap. It provides a set of associated results that describe the benefits of load balancing in cellular networks in high detail, using realistic scenarios and network configurations. At the highest level, the approach is based on a Markov model in which the state at each point in time provides a full description of user connectivity, and the transitions are determined by a range of factors described below. While many previous studies have also applied Markov methods to model network traffic, the approach described here is differentiated from previous work in multiple respects. First, as noted, it incorporates the call admission process, i.e. the process of requesting a connection before the actual assignment of a BS resource. Second, specific consideration is given to

channel quality information, which in turn has a direct effect on the number of successful connections and terminations thereby having an impact on load balancing performance metrics. Third, it incorporates priority differentiation in the load balancing process. We use the prioritization approach, where users that do not have access to multiple base stations get a higher priority in using available cell resources than users that do. More generally, the model allows substantial flexibility with respect to traffic types, admission control, densities of user population, and other parameters, but is also specifically constructed with the function of considering optimal network policy decisions with respect to load balancing.

The rest of the paper is organized as follows. The system model is introduced in Section II, while the analytical model is introduced in Section III. The numerical results are presented in Section IV. Lastly, the paper is concluded in Section V.

## II. SYSTEM MODEL

### A. Channel Structure

We consider a cellular system where two base stations (BSs) are positioned such that they create a region of overlap in coverage. Naturally, while cellular systems typically have far more than two BSs, a reduction to a two-BS system for analytical reasons enables a tractable analytical framework while still allowing exploration of a large number of microscopic parameters to use in optimizing network performance. As our model is of microscopic nature, the extension to a multi-BS system is beyond the scope of this paper. We strongly emphasize that consideration of load balancing in the context of a two-BS system only has been used extensively and successfully in previous treatments, e.g. [4], [7], [13], [14].

Cell 1 has  $M_1$  available basic bandwidth units, as referred to in [15] or more commonly referred to as channels, and cell 2 has  $M_2$  available channels. The throughput of every channel in each cell is the same and equal to  $H$  bits/second. We assume that channels are mutually orthogonal and that there is no interference in the set of channels belonging to cells 1 and 2. Each BS emits a signal using omnidirectional antennas and we assume a circular contour signal coverage model, in which full signal strength is received within a certain radius of the BS, and no signal is available beyond that radius, as used in e.g. [2], [4], [16].

### B. Node Placement

Each mobile terminal, referred to as user equipment (UE), remains at fixed positions following an initial UE placement process, with each UE located in one of three non-overlapping regions as shown

in Fig. 1.  $N_1$  UEs are in group 1 and have access only to one BS,  $N_2$  UEs are in group 2 and have access only to the second BS, and  $N_3$  UEs are in group 3 and can potentially access either BS. Such a non-homogenous UE placement has been considered, for example in [14], which allows for a tractable analysis of the considered system and considers all important groups participating in the load balancing process. The non-homogenous case of UE distribution is the most widespread because UEs are generally distributed non-uniformly over a cellular area. UEs in group 3 are in the region of overlap in coverage between the two cells, also known as the Traffic Transferable Region (TTR) [4]. Since only one UE can occupy a channel at a time, a maximum of  $M_1 + M_2$  UEs can be connected to both cells in the system at any given time. We assume that UEs from groups 1 and 3 are initially registered to cell 1 (serving as the overloaded cell), while UEs in group 2 are initially registered to cell 2.

### C. Signal Transmission Model

Time is slotted and the minimum time unit is a frame length of  $t_s$  seconds. Connections and channel conditions are assumed to remain constant for the duration of a frame, though they will in general vary from frame to frame. Moreover, we assume that the connection and termination processes for UEs are directly dependent on the channel states experienced between each group of UEs and the BSs they are connected to. We also assume that channel states are binary and independent from slot to slot, much as occurs in [17], and that all of the UEs in each group experience the same channel quality to a given BS. Therefore, in any given time slot a UE is either experiencing a good state with probability  $w_{x,y}^{(i)}$ , ( $x$  denotes the particular pair-wise connection between group  $x$  of UEs and associated BS  $y$ , and  $i \in \{d, u\}$  denotes the downlink and uplink, respectively), or a bad state, with probability  $1 - w_{x,y}^{(i)}$ . The value of  $w_{x,y}^{(i)}$  is dependent on the distance between UEs in group  $x$  and BS  $y$ , which is denoted as  $d_{x,y}$ . In our analysis we use the distance as an input to a combined path loss and shadowing propagation model.

### D. Prioritization

Because of the strict boundaries between groups of UEs, we assign priorities on a per group basis. A single, higher priority is given to all UEs in groups 1 and 2 because there is no flexibility to reassign them to a different BS; group 3 UEs can potentially be reassigned and thus given a lower priority. A very similar priority model has been used in other treatments of load balancing. For example, in [13], [18], newly arriving connections in the non-TTR are given first priority to acquire channels from their serving BSs, while the connections from the TTR are assigned to the remaining channels. Our model allows for the implementation of a wide range of scenarios that require such traffic prioritization. One

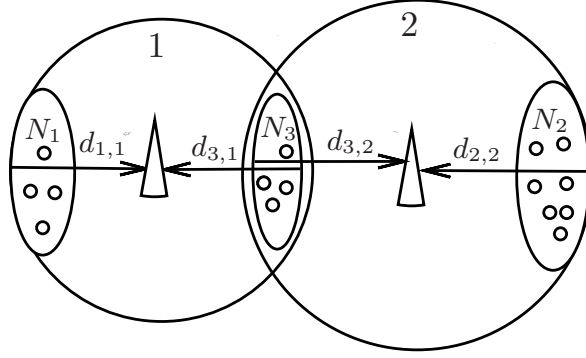


Fig. 1. The system model considered in the analytical evaluation. The two large circles represent two adjacent cells, cell 1 and cell 2, containing 3 groups of UEs. Each UE is indicated by a small circle, and the triangles represent the BSs at the center of each cell. UEs in group 1 have access only to the BS of cell 1, UEs in group 2 have access only to the BS of cell 2, and UEs in group 3 have access to both BSs. The region of overlap between the two cells is referred to as the Traffic Transferable Region.

potential application is for the modeling of networks where load balancing traffic originating from UEs in the TTR has lower priority than non-balanced connections due to several factors including a lower average channel quality [19], [20], QoS requirements [21], non-uniform spatial distribution of traffic classes [14], or cell dwell time. Furthermore, it allows for modeling integrated hybrid cellular/WLAN/Ad Hoc networks as discussed in [6], [22], where non-cellular terminals in the TTR have a lower priority than cellular UEs, and hierarchical cellular systems [23], where members of different tiers have independent priorities. Finally, it enables the modeling of femtocell traffic prioritization, where UEs in groups 1 and 3 are those in the Closed Subscriber Group (CSG) [24], while UEs in the TTR are neighboring UEs outside of the CSG.

#### E. Random Access

In the connection process a UE first attempts to connect to the BS it is initially registered to by requesting a connection through a random access channel. We assume a frequency division duplex transmission mode, where control and data traffic are transmitted and received simultaneously. Each UE generates a connection request with probability  $p_x$ . A connection is requested randomly in one of  $L_x \leq t_s$  non-overlapping, time slotted control resources, unique to group  $x \in \{1, 2, 3\}$  of UEs. In other words, each group has a unique set of sub slots within a frame during which UEs may, but are not required to, request a connection. The random access phase length is equal to slot length  $t_s$ . Collisions between connection requests from UEs in the same group are possible.

The random access procedure considered in this work shares features of the 3GPP-based cellular network standards, which use the Physical Random Access Channel (PRACH), mapped on a one-to-one basis to the logical random access channel (RACH). RACH uses the S-ALOHA protocol and, in relation to the priorities assumed in this paper, allows the prioritization of connection requests based on Active Service Classes (ASC) [10] which are unique to each UE, and can be adapted by the 3GPP-MAC layer once the UE are in connected mode [8, Sec. 2.4.2.6]. The BS advertises itself to the UEs within range through the broadcast channel using signatures (3GPP release 99, e.g. UMTS), subcarriers (3GPP release 8, e.g. LTE), or time slots, which each ASC can in-turn use for connection requests on RACH. The adaptation of the ASC is performed in the time intervals predefined by the operator. For the purpose of our paper we assume that the BSs collectively, through the Radio Network Controller, map the received signal from every registered UE to an associated ASC.

We assume a zero-persistence protocol, i.e. a collision during a connection request implies that connections are lost, and also UEs do not retry to generate another dependent connection. Due to this assumption a power ramping process, i.e. feedback from the UE to the BS on an unsuccessful connection request [10, Sec. II-B], is redundant. To isolate the impact of each group of UEs on collision rates, we assume mutually exclusive RACH resources assigned to each ASC [11, Fig. 4]. Analysis of PRACH performance in isolation can be found in [9], [11].

#### *F. Data Transfer*

A connection request is granted during the connection arrangement process if a good channel state occurs between the UE and its associated BS at the moment of the request, and if no collisions occur between multiple requests from different UEs. Once a connection is established, the BS randomly selects a channel and assigns the connected UE to it. The UE then begins to receive downlink data. UEs terminate a connection with probability  $q$ , where  $1/q = r_p/(Ht_s)$  is the average connection transfer size and  $r_p$  is the average packet size given in bits. We assume that the transfer size is at least one frame long. A connection terminates either when a transmission completes, or when the channel is in a bad state during transmission.

#### *G. Load Balancing Process*

In the case of a UE in group 3, if a connection request is successful and there are no resources available in cell 1, we assume that the radio network controller performs load balancing by transferring the call from cell 1 to cell 2. To avoid overloading cell 2 and protecting UEs that are already registered to it, UEs

in group 3 can access a maximum of  $K$  channels from cell 2, where  $0 \leq K \leq M_2$ . UEs in group 3 have access to an additional  $K$  shared channels, therefore they have access to a total of  $M_1 + K$  channels.

Using the nomenclature of [4, Sec. 2 and 3] this load balancing scheme belongs to a class of direct load balancing schemes. It is closest in operation to direct retry [2]. Since we allow at most  $K$  available channels to offload traffic from cell 1 to cell 2 (as in simple borrowing scheme [4, Sec. 2]) we denote our scheme as *direct retry with truncated offloading channel resource pool* (abbreviated as  $DR_K$ ). With  $K = M_2$  our scheme reduces to classical direct retry, while for  $K = 0$  it reduces to a system in which no load balancing takes place.

In our model we do not use a take-back process. That is, once connections from group 3 are offloaded onto cell 2, they remain connected to cell 2 during the transmission despite whether or not resources have been freed in cell 1. In [5] the authors remark that the take-back process, although more fair to cell 2 because it minimizes blocking at cell 2, is not always advantageous to the network due to the high signaling load that accompanies it. Additionally, as in [4], [16], we do not use queuing, so there is no consideration of a call give-up process [5]. Moreover, we do not allow preemption of connections from the TTR by connections that have access to channels only from their respective BSs.

Note that all variables introduced in this section, as well as all other variables used in this paper are summarized in Table I.

### III. ANALYTICAL MODEL

Let  $\{A, Y^{(1)}, Y^{(2)}, C\}$  denote a state of a Markov system, where  $A$  denotes the number of resources used by group 1 UEs,  $Y^{(1)}$  and  $Y^{(2)}$  denote the number of resources used by group 3 UEs associated with cell 1 and 2, respectively, and  $C$  denotes the number of resources used by group 2 UEs. Then the steady state probabilities can be denoted as  $\pi_{a,b,c,d} \triangleq \Pr(A = a, Y^{(1)} = b, Y^{(2)} = c, C = d)$ . Note that  $a + b + c + d \leq \min\{N_1 + N_2 + N_3, M_1 + M_2\}$ ,  $a + b \leq \min\{N_1 + N_3, M_1\}$ ,  $c + d \leq \min\{N_2 + N_3, M_2\}$ , and  $b + c \leq \min\{N_3, M_1 + K\}$ . These conditions govern what states are possible in the transition probability matrix.

We define the state transition probability as

$$r_{a_{t-1}, b_{t-1}, c_{t-1}, d_{t-1}}^{(a_t, b_t, c_t, d_t)} \triangleq \Pr(A_t = a_t, Y_t^{(1)} = b_t, Y_t^{(2)} = c_t, C_t = d_t | A_{t-1} = a_{t-1}, Y_{t-1}^{(1)} = b_{t-1}, Y_{t-1}^{(2)} = c_{t-1}, C_{t-1} = d_{t-1}), \quad (1)$$

where subscripts  $t$  and  $t - 1$  denote the current and the previous time slots, respectively. This allows for computation of the transition probability matrix required to obtain  $\pi_{a,b,c,d}$ , which is in-turn used to

TABLE I  
SUMMARY OF THE VARIABLES USED IN THE PAPER: FUNCTIONS (TOP) AND VARIABLES (BOTTOM)

Variable	Description	Units
$\{A\}, \{Y^{(1)}, Y^{(2)}\}, \{C\}$	Number of channels used: group 1, 3 (connected to BS 1 and BS 2, resp.) and 2	—
$\pi_{a,b,c,d}$	Steady state probability of the considered Markov chain	—
$r_{a_{t-1}, b_{t-1}, c_{t-1}, d_{t-1}}^{(a_t, b_t, c_t, d_t)}$	Transition probability of the considered Markov chain	—
$(\cdot)\alpha_{(\cdot)}^{(\cdot)}, (\cdot)\theta_{(\cdot)}^{(\cdot)}, (\cdot)\xi_{(\cdot)}^{(\cdot)}$	Functions supporting $r_{a_{t-1}, b_{t-1}, c_{t-1}, d_{t-1}}^{(a_t, b_t, c_t, d_t)}$	—
$P_{S_{x,y}}^{(i)}(\cdot)$	Distribution of $\gamma$ at distance $d_{x,y}$ for $i = \{d, u\}$	—
$w_{x,y}^{(i)}$	Outage probability between group $x$ and BS $y$ in $i = \{d, u\}$	—
$Q(\cdot), I_i^{(j)}$	Q function and indication function, resp.	—
$B^{(x)}, D^{(x)}$	Blocking and collision probability for group $x$ , resp.	—
$S_i^{(j)}, T_i^{(j)}$	Probability of generating, and terminating, $j$ connections given $i$ active users, resp.	—
$\beta_k^{(j)}$	Probability of $j$ successful connections out of $k$ requests on RACH	—
$\tau_{i,x,y}^{(j)}$	Supporting function to compute $S_i^{(j)}$	—
$L_x, L$	Number of access slots assigned to group $x$ , and all groups, resp.	—
$u, d$	Indexes denoting uplink and downlink, resp.	—
$z u, v, i, j, k$	Supporting variables	—
$a, b, c, d$	Channels occupied: group 1, group 3 (connected to BS 1 and BS 2, resp.), group 2	—
$t, t-1$	Current and previous time slots indexes, resp.	—
$t_s$	Frame length	seconds
$\gamma_q^{(i)}$	Signal reception threshold for $i = \{u, d\}$	dB
$\gamma$	Received signal level	dB
$\delta, \sigma_\Psi$	Pathloss exponent and shadowing variance, resp.	—
$J_{x,y}^{(i)}$	Received signal at $i = \{d, u\}$ for UE group $x$ and BS $y$	—
$p_x, p$	Probability of connection request generation by UE group $x$ , and all groups, resp.	—
$d_{x,y}, d_{0,x,y}^{(i)}$	Normal and reference distance for $i = \{u, d\}$ used in pathloss calculations, resp.	m
$H$	Individual channel throughput	b/s
$K$	Fraction of channels in BS 2	—
$U$	Channel utilization	—
$W^{(i)}$	Unit-less constant used in pathloss calculation for $i = \{u, d\}$	—
$P_t^{(i)}$	Transmitted power by BS ( $i = d$ ) and UE ( $i = u$ )	dB
$M_y, N_x$	Number of channels used by BS $y$ and number of UEs in group $x$ , resp.	—
$l_{x,y}$	Average packet length, given channel quality transmitted, from BS $y$ to UE group $x$	frames
$1/q, r_p$	Average packet length in perfect channel conditions	frames, bits
$b^{(i)}, d^{(i)}$	Required probability of blocking and collision, respectively, for group $x$	—
$g_a, g_c, g_d, g_e, i_a, i_d$	Variables and functions supporting $B^{(x)}$	—
$\eta$	Variable supporting $D^{(x)}$	—



compute the performance metrics of the load balancing-enabled cellular system. In the subsequent sections we describe the process of deriving the transition probability  $r_{a_{t-1}, b_{t-1}, c_{t-1}, d_{t-1}}^{(a_t, b_t, c_t, d_t)}$ . We begin by explaining the computation process for the channel quality, and then focus on the derivation of the functions that support (1).

#### A. Derivation of Channel Quality

In the downlink, the probability of a UE belonging to group  $x \in \{1, 2, 3\}$  and receiving a good signal from BS  $y \in \{1, 2\}$ , is defined as

$$w_{x,y}^{(d)} \triangleq 1 - \Pr(J_{x,y}^{(d)} \leq \gamma_q^{(d)}) = 1 - \int_0^{\gamma_q^{(d)}} p_{S_{x,y}^{(d)}}(\gamma, d_{x,y}) d\gamma, \quad (2)$$

where  $\gamma_q^{(d)}$  is the signal reception threshold for the downlink, expressed as the minimum required received power of the received signal  $J_{x,y}^{(d)}$ , and  $p_{S_{x,y}^{(d)}}(\gamma, d_{x,y})$  is the distribution of the signal  $\gamma$  received at group  $x$ , which is at a distance of  $d_{x,y}$  from BS  $y$ . As an example, we consider an environment with path loss and shadowing, where  $w_{x,y}^{(d)}$  is expressed in [25, Eq. 2.25] as

$$w_{x,y}^{(d)} = Q \left( \frac{\gamma_q^{(d)} - P_t^{(d)} - 10 \log_{10} W^{(d)} + 10\delta \log_{10} \frac{d_{x,y}}{d_{0,x,y}^{(d)}}}{\sigma_\Psi} \right), \quad (3)$$

where  $W^{(d)}$  is a unit-less constant dependent on both the antenna characteristics and an average channel attenuation, given as [25, Eq. 2.41],  $P_t^{(d)}$  is the BS transmitted power (which is assumed to be the same for both base stations),  $d_{x,y}$  is the distance of the UE in group  $x$  located furthest from BS  $y$ ;  $d_{0,x,y}^{(d)}$  is the reference distance for the BS antenna far-field;  $\sigma_\Psi$  is the log-normal shadowing variance given in dB;  $\delta$  is the path loss exponent; and the  $Q$  function is defined in the usual manner as

$$Q(z) \triangleq \int_z^\infty \frac{1}{\sqrt{2\pi}} e^{-u^2/2} du. \quad (4)$$

In the uplink, the probability that a good signal is received by BS  $y$  from a UE in group  $x$  is  $w_{x,y}^{(u)}$ , and is expressed in the same manner as equations (2) and (3), by replacing all variables having superscript  $(d)$  with  $(u)$ , where  $P_t^{(u)}$  denotes the UE transmission power;  $W^{(u)}$  denotes the constant for the UE antenna;  $d_{0,x,y}^{(u)}$  is the reference distance for the UE antenna far-field; and  $\gamma_q^{(u)}$  is the signal reception threshold for the uplink. The downlink and uplink channel quality information governs the success rate of the connection admission process, as well as the duration of a downlink transmission.

### B. Derivation of Connection Arrangement Probability

An important feature of the model is the consideration of connection admission in the load-balancing process. This process is a function of the total number of UEs, the number of UEs receiving data from their respective serving BSs, the pairwise channel quality between the UEs and its serving BSs, and the underlying random access algorithm. The probability that  $j$  new connections have successfully requested downlink data given  $i_{t-1} \in \{a_{t-1}, b_{t-1}, c_{t-1}, d_{t-1}\}$  currently active connections from group  $x$ , with a random access channel consisting of  $L_x$  time slots is

$$S_{i_{t-1}}^{(j)} \triangleq \begin{cases} \tau_{i_{t-1},x,y}^{(i_t)}, & j > 0, \\ 1 - w_{x,y}^{(u)} + \tau_{i_{t-1},x,y}^{(1)}, & j = 0, \\ 0, & \text{otherwise,} \end{cases} \quad (5)$$

where

$$\tau_{i_{t-1},x,y}^{(j)} \triangleq w_{x,y}^{(u)} \sum_{k=j}^{N_x - i_{t-1}} \binom{N_x - i_{t-1}}{k} p_x^k (1 - p_x)^{N_x - i_{t-1} - k} \beta_k^{(j)}; \quad (6)$$

$p_x$  is the probability of a connection request by an individual UE in group  $x$ ; and  $\beta_k^{(j)}$  is the probability that among  $k$  UEs requesting a connection,  $j$  were successful in obtaining a resource. Note that the reference to  $x, y$  in  $S_{i_{t-1}}^{(j)}$  is omitted due to space constraints, keeping in mind that for  $a_t, a_{t-1}$   $x = 1$ ,  $y = 1$ , for  $b_t, b_{t-1}$   $x = 3$ ,  $y = 1$ , for  $c_t, c_{t-1}$   $x = 3$ ,  $y = 2$ , and for  $d_t, d_{t-1}$   $x = 2$ ,  $y = 2$ .

For consistency with cellular networks such as 3GPP, we consider a PRACH-like control channel, for which  $\beta_k^{(j)}$  can be described in the manner of [26, Eq. (3)]

$$\beta_k^{(j)} = \sum_{m=j}^{\min(k, L_x)} \frac{(-1)^{m+j} (L_x - m)^{k-m} k!}{(m-j)!(L_x - m)!(k-m)!n!}. \quad (7)$$

Note that depending on the assumption of how collisions are resolved, different definitions of  $\beta_k^{(j)}$  in equation (7) can be applied when calculating the connection arrangement probability according to (5).

### C. Connection Termination Probability

Once a UE successfully requests a connection from the serving BS, a downlink transmission is started provided that at least one free channel is available for the UE. The connection terminates when the BS finishes transmitting data to the UE or when the downlink signal received by the UE is in outage. The probability that  $j$  connections from  $i_{t-1}$  active connections at group  $x$  terminate is

$$T_{i_{t-1}}^{(j)} \triangleq \binom{i_{t-1}}{j} l_{x,y}^j (1 - l_{x,y})^{i_{t-1} - j}, \quad (8)$$

where  $l_{x,y} = 1 - w_{x,y}^{(d)} + w_{x,y}^{(d)}q$  is the inverse of the average packet length, accounting for truncation of some packets due to a bad channel quality. Again, the indices  $x, y$  have been omitted for notational simplicity in the symbol  $T_{i_{t-1}}^{(j)}$ , assuming that the same relationship between  $x, y$  and  $j, i_{t-1}$  as given in Section III-B holds.

#### D. Derivation of the State Transition Probability

Using the definitions of the arrangement and termination probabilities, expressed in (5) and (8), respectively, we can finally introduce the state transition probabilities for the complete model. The transition probability is constructed using the termination and arrangement probability definitions and the respective relationship between the variables of these two definitions (which are dependent on the start and end states of the transition). Due to the complexity of the derivation we begin with a highly simplified example.

1) *State Transition Probabilities for a Single UE Group:* To facilitate understanding the derivation of the complete state transition probabilities, we first consider a network in which no load balancing occurs and all of the UEs are in group 1, such that  $N_1 > 0$  and  $N_2 = N_3 = 0$ . The state of the Markov chain then simplifies to  $\{A, 0, 0, 0\}$  and the transition probability becomes  $r_{a_{t-1}, 0, 0, 0}^{(a_t, 0, 0, 0)}$ , where

$$r_{a_{t-1}, 0, 0, 0}^{(a_t, 0, 0, 0)} = \begin{cases} \sum_{i=0}^{a_t} T_{a_{t-1}}^{(i+a_{t-1}-a_t)} S_{a_{t-1}}^{(i)}, & a_{t-1} \geq a_t, a_t \neq M_1, \\ \sum_{i=0}^{a_t} T_{a_{t-1}}^{(i)} S_{a_{t-1}}^{(i+a_t-a_{t-1})}, & a_{t-1} < a_t, a_t \neq M_1, \\ \sum_{i=0}^{a_t} T_{a_{t-1}}^{(i)} S_{a_{t-1}}^{(i+a_t-a_{t-1})} \\ + \sum_{i=0}^{a_t} T_{a_{t-1}}^{(i)} \sum_{j=M_1}^{N_1} S_{a_{t-1}}^{(i+j-a_{t-1})}, & a_{t-1} \leq a_t, a_t = M_1. \end{cases} \quad (9)$$

In (9) the case  $a_{t-1} \geq a_t, a_t \neq M_1$  denotes the transition from a higher to a lower channel occupancy, subject to the constraint that the number of channels occupied in the end state can not exceed the total BS capacity. The number of terminating UEs is set to compensate for the UEs that generate successful connections. The case  $a_{t-1} < a_t, a_t \neq M_1$  denotes the transition from a lower to a higher channel occupancy (given, again, that the number of occupied channels is less than the total BS capacity). In this case UEs from group 1 need to generate exactly as many connections as given by the end state, not forgetting to generate connections in order to compensate for the total number of terminations. Lastly, for the case of  $a_{t-1} \leq a_t, a_t = M_1$  the end state equals the total channel capacity. The first term in the definition of this transition probability includes exactly the number of connections needed to reach the end state, once again compensating for terminations. The second term accounts for all successful connections generated that exceed those needed to reach the end state, which will not be admitted.

2) *General Solution for the State Transition Probabilities:* As expected, the current state of the UEs in each group has a strong impact on the allowable future states in all groups. For example, newly generated connections from UEs in group 2 are initially assigned to cell 1 and can only be offloaded to cell 2 once all channels on cell 1 are occupied. Therefore, in the process of constructing the complete set of transition probabilities, not only is it necessary to enumerate all conditions that govern these possible transitions, as in (9), but it is also important to consider the relationship between the possible combinations of termination and arrangement probabilities.

Before presenting the general solution, we introduce supporting functions that simplify the description of the transition probabilities. First, because the system is composed of three groups, where groups 1 and 2 have the same level of priority, we define a function that governs the transition probabilities for these groups, i.e.

$$(M_i, N_j) \alpha_{i_{t-1}, j_{t-1}}^{(i_t, z)} \triangleq \begin{cases} \sum_{k=0}^{i_t} T_{i_{t-1}}^{(k+i_{t-1}-i_t)} S_{i_{t-1}}^{(i)}, & i_t + j_t \leq M_i, i_t < i_{t-1}; \\ \sum_{k=0}^{i_t} T_{i_{t-1}}^{(k)} S_{i_{t-1}}^{(k+i_{t-1}-i_t)}, & i_t + j_t < M_i, i_t \geq i_{t-1} \text{ or} \\ \sum_{k=0}^{i_t} T_{i_{t-1}}^{(k)} S_{i_{t-1}}^{(k+i_t-i_{t-1})} & i_t + j_t = M_i, i_t \geq i_{t-1}, j_t > j_{t-1}; \\ + I_{j_{t-1}-z+i_t}^{(M_i)} & \\ \times T_{i_{t-1}}^k \sum_{n=i_t+1}^{N_j} S_{i_{t-1}}^{(k+n-i_{t-1})}; & i_t + j_t = M_i, i_t \geq i_{t-1}, j_t \leq j_{t-1}. \end{cases} \quad (10)$$

where  $I_i^{(j)} = 1$  when  $i \geq j$  and  $I_i^{(j)} = 0$ , otherwise. Variables  $i_x$  and  $j_x$  are supporting parameters that will be replaced by respective variables of (1), once we derive general formulas for transition probabilities. The ranges of  $i_x$  and  $j_x$  will be defined in the respective transition probabilities shown later. Note that (10) resembles (9), except for the introduction of the indicator function  $I_i^{(j)}$ . For the remaining groups, we define the following supporting functions which denote the possible termination probabilities for group

3

$${}^{(n)}\theta_{b_{t-1}, c_{t-1}}^{(b_t, c_t, k, l)} \triangleq \begin{cases} T_{b_{t-1}}^{(k)} T_{c_{t-1}}^{(l)}, & n = 1, \\ T_{b_{t-1}}^{(k+b_{t-1}-b_t)} T_{c_{t-1}}^{(l+c_{t-1}-c_t)}, & n = 2, \\ T_{b_{t-1}}^{(k+b_{t-1}-b_t)} T_{c_{t-1}}^{(l)}, & n = 3, \\ T_{b_{t-1}}^{(k)} T_{c_{t-1}}^{(l+c_{t-1}-c_t)}, & n = 4. \end{cases} \quad (11)$$

Note that the termination probabilities for group 3 in (11) are composed of individual termination function as given in (8). One reason for this is that different channel qualities are experienced by UEs in the TTR, resulting in unequal termination probabilities, depending on whether these UEs are connected to BS 1

or BS 2. Lastly, we define

$${}^{(n)}\xi_{b_{t-1},c_{t-1}}^{(b_t,c_t,k,l)} \triangleq \begin{cases} S_{b_{t-1}+c_{t-1}}^{(k+l+b_t+c_t-b_{t-1}-c_{t-1})}, & n = 1, \\ S_{b_{t-1}+c_{t-1}}^{(k+l)}, & n = 2, \\ S_{b_{t-1}+c_{t-1}}^{(k+l+c_t-c_{t-1})}, & n = 3, \\ S_{b_{t-1}+c_{t-1}}^{(k+l+b_t-b_{t-1})}, & n = 4. \end{cases} \quad (12)$$

which denotes the possible arrangement probabilities for group 3. Note that the variables  $k$ ,  $l$  and  $z$  in (10), (11) and (12) are the enumerators. Given the above, we can identify two major states of the system as follows: when all channels are occupied on both cells (called an edge state and having the same meaning as the last condition in (9)); and the remaining states. We start by describing the edge state conditions.

3) *Edge state*: Here we list the following sub-cases. For  $a_t + b_t = M_1$ ,  $c_t + d_t = M_2$ ,  $b_t \geq b_{t-1}$ ,  $c_t \geq c_{t-1}$  or  $a_t + b_t = M_1$ ,  $c_t + d_t < M_2$ ,  $b_t \geq b_{t-1}$ ,  $c_t \geq c_{t-1}$ ,  $c_t = K$  we have

$$\begin{aligned} r_{a_{t-1},b_{t-1},c_{t-1},d_{t-1}}^{(a_t,b_t,c_t,d_t)} &= \sum_{k=0}^{b_{t-1}} \sum_{l=0}^{c_{t-1}} \left( {}^{(1)}\theta_{b_{t-1},c_{t-1}}^{(b_t,c_t,k,l)} {}^{(1)}\xi_{b_{t-1},c_{t-1}}^{(b_t,c_t,k,l)} + {}^{(1)}\theta_{b_{t-1},c_{t-1}}^{(b_t,c_t,k,l)} \right. \\ &\quad \times \sum_{r=l+1}^{N_3} {}^{(1)}\xi_{b_{t-1},c_{t-1}}^{(b_t,c_t,k,r)} \Big)_{(M_1,N_1)} \alpha_{a_{t-1},b_{t-1}}^{(a_t,k)} {}_{(M_2,N_2)} \alpha_{d_{t-1},c_{t-1}}^{(d_t,l)}. \end{aligned} \quad (13)$$

Equation (13) holds when the number of connections from group 3 UEs to both BS 1 and BS 2 increases. The first term in the brackets enumerates all the possible cases of terminations and generations in group 3 given a certain starting state. The second term in the brackets accounts for the edge case. This condition is similar in nature to the third case in (9). Lastly, the remaining  $(\cdot)\alpha_{(\cdot)}^{(\cdot)}$  terms account for the possible transitions in group 1 and 2. The indicator function used in the last condition of (10) is a function of the termination and connection enumerators in group 3. That is, depending on how many connections are admitted in BS 1 and BS 2 in a previous frame, a certain number of UEs from group 1 and 2 that request connections will not be admitted.

For  $a_t + b_t = M_1$ ,  $c_t + d_t = M_2$ ,  $b_t < b_{t-1}$ ,  $c_t < c_{t-1}$  or  $a_t + b_t = M_1$ ,  $c_t + d_t = M_2$ ,  $b_t = b_{t-1}$ ,  $c_t < c_{t-1}$  or  $a_t + b_t = M_1$ ,  $c_t + d_t = M_2$ ,  $b_t < b_{t-1}$ ,  $c_t = c_{t-1}$  or  $a_t + b_t = M_1$ ,  $c_t + d_t < M_2$ ,  $b_t < b_{t-1}$ ,  $c_t = c_{t-1} = K$  we have

$$\begin{aligned} r_{a_{t-1},b_{t-1},c_{t-1},d_{t-1}}^{(a_t,b_t,c_t,d_t)} &= \sum_{k=0}^{b_t} \sum_{l=0}^{c_t} \left( {}^{(2)}\theta_{b_{t-1},c_{t-1}}^{(b_t,c_t,k,l)} {}^{(2)}\xi_{b_{t-1},c_{t-1}}^{(b_t,c_t,k,l)} + {}^{(2)}\theta_{b_{t-1},c_{t-1}}^{(b_t,c_t,k,l)} \right. \\ &\quad \times \sum_{r=l+1}^{N_3} {}^{(2)}\xi_{b_{t-1},c_{t-1}}^{(b_t,c_t,k,r)} \Big)_{(M_1,N_1)} \alpha_{a_{t-1},b_{t-1}}^{(a_t,k+b_{t-1}-b_t)} {}_{(M_2,N_2)} \alpha_{d_{t-1},c_{t-1}}^{(d_t,l+c_{t-1}-c_t)}. \end{aligned} \quad (14)$$

In this case the number of connections from group 3 to both BS 1 and BS 2 decreases, or the number of connections in any one of the BSs remains the same, while the other decreases. The construction of the transition probability is the same as in (13), respectively replacing  $^{(1)}\theta_{(\cdot)}^{(\cdot)}$  with  $^{(2)}\theta_{(\cdot)}^{(\cdot)}$ . Note that the definition of  $^{(2)}\theta_{(\cdot)}^{(\cdot)}$  in (11) defines the number of freed connections at BS 1 and BS 2 because of terminations of group 3 UEs. Since the number of connections have to be maintained at full cell occupancy for cell 1 and cell 2, the respective functions  $_{(\cdot)}\alpha_{(\cdot)}^{(\cdot)}$  for BS 1 and BS 2, are used to compensate for the possible number of terminations at each cell due to group 3 UEs in order to maintain full system-wide occupancy, i.e. to remain at the edge state.

For  $a_t + b_t = M_1$ ,  $c_t + d_t = M_2$ ,  $b_t < b_{t-1}$ ,  $c_t > c_{t-1}$  or  $a_t + b_t = M_1$ ,  $c_t + d_t < M_2$ ,  $b_t < b_{t-1}$ ,  $c_t > c_{t-1}$ ,  $c_t = K$

$$r_{a_{t-1}, b_{t-1}, c_{t-1}, d_{t-1}}^{(a_t, b_t, c_t, d_t)} = \sum_{k=0}^{b_t} \sum_{l=0}^{c_{t-1}} \left( {}^{(3)}\theta_{b_{t-1}, c_{t-1}}^{(b_t, c_t, k, l)} {}^{(3)}\xi_{b_{t-1}, c_{t-1}}^{(b_t, c_t, k, l)} + {}^{(3)}\theta_{b_{t-1}, c_{t-1}}^{(b_t, c_t, k, l)} \right. \\ \left. \times \sum_{r=l+1}^{N_3} {}^{(3)}\xi_{b_{t-1}, c_{t-1}}^{(b_t, c_t, k, r)} \right) (M_1, N_1) \alpha_{a_{t-1}, b_{t-1}}^{(a_t, k + b_{t-1} - b_t)} (M_2, N_2) \alpha_{d_{t-1}, c_{t-1}}^{(d_t, l)}. \quad (15)$$

This case describes the situation where the number of connections from group 3 UEs to BS 1 strictly decreases, while those from group 3 UEs to BS 2 strictly increases. The transition probability represented in (13) can account for this by replacing  $^{(1)}\theta_{(\cdot)}^{(\cdot)}$  with  $^{(3)}\theta_{(\cdot)}^{(\cdot)}$ . The definition of  $^{(3)}\theta_{(\cdot)}^{(\cdot)}$  from (11) describes the case when the number of terminations at BS 1 from group 3 UEs account for the decrease in the number of connections, while the number of terminations at BS 2 account only for any additional number of generations. The respective function  $_{(\cdot)}\alpha_{(\cdot)}^{(\cdot)}$  for BS 1 and BS 2, again, must compensate for the changes in connections from group 3 to BS 1 and BS 2 in order to maintain full-cell occupancy. Lastly, for  $a_t + b_t = M_1$ ,  $c_t + d_t = M_2$ ,  $b_t > b_{t-1}$ ,  $c_t < c_{t-1}$

$$r_{a_{t-1}, b_{t-1}, c_{t-1}, d_{t-1}}^{(a_t, b_t, c_t, d_t)} = \sum_{k=0}^{b_{t-1}} \sum_{l=0}^{c_t} \left( {}^{(4)}\theta_{b_{t-1}, c_{t-1}}^{(b_t, c_t, k, l)} {}^{(4)}\xi_{b_{t-1}, c_{t-1}}^{(b_t, c_t, k, l)} + {}^{(4)}\theta_{b_{t-1}, c_{t-1}}^{(b_t, c_t, k, l)} \right. \\ \left. \times \sum_{r=l+1}^{N_3} {}^{(4)}\xi_{b_{t-1}, c_{t-1}}^{(b_t, c_t, k, r)} \right) (M_1, N_1) \alpha_{a_{t-1}, b_{t-1}}^{(a_t, k)} (M_2, N_2) \alpha_{d_{t-1}, c_{t-1}}^{(d_t, l + c_{t-1} - c_t)}. \quad (16)$$

The above case is the opposite of that in (15). Here, the number of connections from group 3 to BS 1 strictly increases, while those from group 3 to BS 2 strictly decreases. Again, respective expressions for  $^{(1)}\theta_{(\cdot)}^{(\cdot)}$  in (13) need to be replaced by  $^{(4)}\theta_{(\cdot)}^{(\cdot)}$ . The explanation for  $^{(4)}\theta_{(\cdot)}^{(\cdot)}$  and  $_{(\cdot)}\alpha_{(\cdot)}^{(\cdot)}$  given in (11) is equivalent to the explanation for (15).

4) *Non-Edge state*: The second major group of cases refers to the situation in which the number of connections at BS 1 or BS 2 is less than or equal to the maximum capacity. This obviously involves

more cases to consider than those explained in Section III-D3. We start by denoting conditions under which a transition from one state to another is not possible. That is, for  $a_t + b_t < M_1$ ,  $c_t + d_t \leq M_2$ ,  $b_t > b_{t-1}$ ,  $c_t > c_{t-1}$  or  $a_t + b_t < M_1$ ,  $c_t + d_t \leq M_2$ ,  $b_t < b_{t-1}$ ,  $c_t > c_{t-1}$

$$r_{a_{t-1}, b_{t-1}, c_{t-1}, d_{t-1}}^{(a_t, b_t, c_t, d_t)} = 0. \quad (17)$$

For  $a_t + b_t < M_1$ ,  $c_t + d_t \leq M_2$ ,  $b_t > b_{t-1}$ ,  $c_t = c_{t-1}$

$$r_{a_{t-1}, b_{t-1}, c_{t-1}, d_{t-1}}^{(a_t, b_t, c_t, d_t)} = \sum_{k=0}^{b_{t-1}} (1) \theta_{b_{t-1}, c_{t-1}}^{(b_t, c_t, k, 0)} (1) \xi_{b_{t-1}, c_{t-1}}^{(b_t, c_t, k, 0)} (M_1, N_1) \alpha_{a_{t-1}, b_{t-1}}^{(a_t, k)} (M_2, N_2) \alpha_{d_{t-1}, c_{t-1}}^{(d_t, 0)}. \quad (18)$$

The above case is partially equivalent to (13) and considers the situation where the number of connections of group 3 UEs connected to BS 1 increases and those to BS 2 stay the same. Also, the number of new connections at BS 1 is less than its maximum capacity. Since this is not an edge case for the system, an additional third summation term is not needed as seen in (13). Note that this condition only contains one summation because the number of terminations from UEs connected to BS 2 cannot exceed the resultant connection state. This is because if they do exceed the desired number of terminations, UEs that generate connections to compensate for additional terminations will instead choose to connect to BS 1 (the BS they are registered to) thereby changing the resultant connection state. Now, for  $a_t + b_t = M_1$ ,  $c_t + d_t < M_2$ ,  $b_t \geq b_{t-1}$ ,  $c_t \geq c_{t-1}$

$$r_{a_{t-1}, b_{t-1}, c_{t-1}, d_{t-1}}^{(a_t, b_t, c_t, d_t)} = \sum_{k=0}^{b_{t-1}} \sum_{l=0}^{c_{t-1}} (1) \theta_{b_{t-1}, c_{t-1}}^{(b_t, c_t, k, l)} (1) \xi_{b_{t-1}, c_{t-1}}^{(b_t, c_t, k, l)} (M_1, N_1) \alpha_{a_{t-1}, b_{t-1}}^{(a_t, k)} (M_2, N_2) \alpha_{d_{t-1}, c_{t-1}}^{(d_t, l)}. \quad (19)$$

This case is an extension of the case described in (18). However, full-cell occupancy now occurs at BS 1, i.e. all channels of BS 1 are occupied after the transition, and BS 2 operates at less than its maximum capacity. An additional summation is used as compared to (18) because full-cell occupancy on BS 1 allows for terminations to occur on BS 2 from group 3 UEs without changing their resultant connection number. Now, for  $a_t + b_t < M_1$ ,  $c_t + d_t \leq M_2$ ,  $c_t < c_{t-1}$ ,  $b_t < b_{t-1}$ , or  $a_t + b_t = M_1$ ,  $c_t + d_t < M_2$ ,  $b_t = b_{t-1}$ ,  $c_t < c_{t-1}$  or  $a_t + b_t = M_1$ ,  $c_t + d_t < M_2$ ,  $b_t < b_{t-1}$ ,  $c_t = c_{t-1}$

$$r_{a_{t-1}, b_{t-1}, c_{t-1}, d_{t-1}}^{(a_t, b_t, c_t, d_t)} = \sum_{k=0}^{b_{t-1}} (2) \theta_{b_{t-1}, c_{t-1}}^{(b_t, c_t, k, 0)} (2) \xi_{b_{t-1}, c_{t-1}}^{(b_t, c_t, k, 0)} (M_1, N_1) \alpha_{a_{t-1}, b_{t-1}}^{(a_t, k+b_{t-1}-b_t)} (M_2, N_2) \alpha_{d_{t-1}, c_{t-1}}^{(d_t, c_{t-1}-c_t)}. \quad (20)$$

The case described by (20) is a direct extension of (14). Similar to (18), terminations from group 3 UEs to BS 2 cannot be considered to achieve the resultant connection state. Next, for  $a_t + b_t = M_1$ ,  $c_t + d_t < M_2$ ,  $b_t < b_{t-1}$ ,  $c_t < c_{t-1}$  or  $a_t + b_t = M_1$ ,  $c_t + d_t < M_2$ ,  $b_t = b_{t-1}$ ,  $c_t < c_{t-1}$  or  $a_t + b_t = M_1$ ,

$$c_t + d_t < M_2, b_t < b_{t-1}, c_t = c_{t-1}$$

$$r_{a_{t-1}, b_{t-1}, c_{t-1}, d_{t-1}}^{(a_t, b_t, c_t, d_t)} = \sum_{k=0}^{b_t} \sum_{l=0}^{c_{t-1}} (2) \theta_{b_{t-1}, c_{t-1}}^{(b_t, c_t, k, l)} (2) \xi_{b_{t-1}, c_{t-1}}^{(b_t, c_t, k, l)} \times (M_1, N_1) \alpha_{a_{t-1}, b_{t-1}}^{(a_t, k+b_{t+1}-b_t)} (M_2, N_2) \alpha_{d_{t-1}, c_{t-1}}^{(d_t, l+c_{t+1}-c_t)}. \quad (21)$$

The above case is an extension of the transition probability described in (20). It considers the situation when full-cell occupancy occurs only at BS 1. Next, for  $a_t + b_t = M_1, c_t + d_t < M_2, b_t < b_{t-1}, c_t > c_{t-1}$

$$r_{a_{t-1}, b_{t-1}, c_{t-1}, d_{t-1}}^{(a_t, b_t, c_t, d_t)} = \sum_{k=0}^{b_t} \sum_{l=0}^{c_{t-1}} (3) \theta_{b_{t-1}, c_{t-1}}^{(b_t, c_t, k, l)} (3) \xi_{b_{t-1}, c_{t-1}}^{(b_t, c_t, k, l)} (M_1, N_1) \alpha_{a_{t-1}, b_{t-1}}^{(a_t, k+b_{t+1}-b_t)} (M_2, N_2) \alpha_{d_{t-1}, c_{t-1}}^{(d_t, l)}. \quad (22)$$

The above case is an extension of the case described by (15). However, only full cell occupancy at BS 1 is considered. Next, for  $a_t + b_t < M_1, c_t + d_t \leq M_2, b_t > b_{t-1}, c_t < c_{t-1}$

$$r_{a_{t-1}, b_{t-1}, c_{t-1}, d_{t-1}}^{(a_t, b_t, c_t, d_t)} = \sum_{k=0}^{b_t} (4) \theta_{b_{t-1}, c_{t-1}}^{(b_t, c_t, k, 0)} (4) \xi_{b_{t-1}, c_{t-1}}^{(b_t, c_t, k, 0)} (M_1, N_1) \alpha_{a_{t-1}, b_{t-1}}^{(a_t, k)} (M_2, N_2) \alpha_{d_{t-1}, c_{t-1}}^{(d_t, c_{t-1}-c_t)}. \quad (23)$$

The above case is an extension of (16). In the case of (23) full-cell occupancy does not occur in any of the cells, therefore the respective summation terms from (16) accounting for the edge case are removed. Also, there is only one summation because as in (18) and (20) terminations from group 3 UEs to BS 2 cannot be considered to achieve the desired end state. Lastly, for  $a_t + b_t = M_1, c_t + d_t < M_2, b_t > b_{t-1}, c_t < c_{t-1}$

$$r_{a_{t-1}, b_{t-1}, c_{t-1}, d_{t-1}}^{(a_t, b_t, c_t, d_t)} = \sum_{k=0}^{b_{t-1}} \sum_{l=0}^{c_t} (4) \theta_{b_{t-1}, c_{t-1}}^{(b_t, c_t, k, l)} (4) \xi_{b_{t-1}, c_{t-1}}^{(b_t, c_t, k, l)} (M_1, N_1) \alpha_{a_{t-1}, b_{t-1}}^{(a_t, k)} (M_2, N_2) \alpha_{d_{t-1}, c_{t-1}}^{(d_t, l+c_{t-1}-c_t)}. \quad (24)$$

The final case is an extension of the case described by (23). However, it considers the case when full cell occupancy occurs only at BS 1.

### E. Performance Metrics

Given the complete description of the system, we are able to derive important metrics that would describe the efficiency of the load balancing process involving connection admission. While there are many performance metrics that can be extracted given the above framework, we focus on three primary metrics: (i) the blocking probability, which describes the probability that at least one UE which requests a connection from a particular group will be denied access to a channel, (ii) the channel utilization, which expresses the fraction of the available channels are being used, and (iii) the collision probability on a control channel, which provides the probability that at least one requesting connection will be lost due to a collision with another UE.



1) *Blocking Probability*: As used here, blocking occurs when at least one UE requests a new connection, but cannot be admitted to any BS due to lack of available channels. Since each group has access to a different number of channels and can follow a different connection strategy, it is necessary to define separate blocking probability metrics for UEs in groups 1 and 2, as contrasted with UEs in group 3. For groups 1 and 2, the blocking probability is defined according to

$$B^{(z)} = \sum_{a,b,c,d} \sum_{i=0}^x \sum_{j=M_v-x-y+1}^{N_z} \sum_{k=0}^y \pi_{a,b,c,d} T_x^{(i)} T_y^{(k)} S_x^{(i+j+k)}, \quad (25)$$

where for  $z = 1$   $x = a$ ,  $y = b$ ,  $v = 1$  and for  $z = 3$   $x = d$ ,  $y = c$ ,  $v = 2$ . For group 3 UEs, the blocking probability is given as

$$B^{(3)} = \sum_{a,b,c,d} \sum_{i_a=0}^a \sum_{j_a=0}^{N_1} \sum_{i_d=0}^d \sum_{j_d=0}^{N_3} \sum_{i=0}^b \sum_{j=0}^c \sum_{k=\phi}^{N_2} \pi_{a,b,c,d} T_a^{(i_a)} S_a^{(j_a)} T_d^{(j_d)} S_d^{(j_d)} T_b^{(i)} T_c^{(j)} S_{b+c}^{(i+j+k)}, \quad (26)$$

where  $\phi$  is defined separately for  $K < M_2$  and  $K = M_2$ . For  $K = M_2$   $\phi = M_1 + M_2 - a - b - c - d - g_a - g_d + i_a + i_d + 1$ , where

$$g_a = \begin{cases} M_1 - a + i_a - b + i, & j_a > M_1 - a + i_a - b + i, \\ j_a, & \text{otherwise,} \end{cases} \quad (27)$$

and  $g_d$  is defined as (27) replacing  $M_1$  with  $M_2$ ,  $a$  with  $c$ ,  $i_a$  with  $i_d$ ,  $b$  with  $d$  and  $i$  with  $j$ . For  $K < M_2$   $\phi = M_1 - g_a - b - j_a + i_a + i + g_c + 1$ , where  $g_a$  is defined as (27) and

$$g_c = \begin{cases} \max\{0, g_e\}, & g_e < K \\ K - c + j, & c - j < K \text{ and } g_e \geq K, \\ 0, & \text{otherwise,} \end{cases} \quad (28)$$

where  $g_e = M_2 - c - d + i_d + j - j_d$ .

We briefly explain the above equations. The derivation of the blocking probability for group 3 UEs is more complicated than for those UEs in groups 1 and 2 because this group can access channels from both cells. Therefore, the number of generations for group 3 UEs that leads to blocking has to account for the terminations within the same group, and also for the possible changes in the number of connections of UEs in groups 1 and 2.

The blocking for group 3 UEs can be analyzed in two separate cases. The first case accounts for the number of generations needed to occupy all the channels in cell 1 ( $K = M_2$ ), while the second case accounts for the number of generations needed to occupy all available channels in cell 2 ( $K < M_2$ ). The first case is simpler to analyze because group 3 UEs need only generate as many connections as there are available resources on cell 1.

When  $K < M_2$ , group 3 UEs can only access a maximum of  $K$  channels on cell 2. Therefore, extra conditions are added for the situation in which group 3 UEs are blocked when exceeding  $K$  connections in cell 2. If there are less than  $K$  available free channels after terminations of group 3 UEs connected to cell 2, the function  $\max\{0, g_e\}$  represents the number of connections to cause blocking by generating the exact number of connections to occupy all available channels. The  $\max\{0, g_e\}$  function is used to lower bound the necessary number of connections for blocking. This is because the number of connections on cell 2, in general, is not restricted to  $K$  and can thus have more than  $K$  current occupancies resulting in a possibly negative value for  $g_e$ . On the other hand, if there are more than  $K$  available channels after terminations, exactly  $K$  channels are used by group 3 UEs to cause blocking.

2) *Channel Utilization and Total System Throughput*: The overall channel utilization is

$$U = \frac{1}{M_1 + M_2} \sum_{a,b,c,d} (a + b + c + d) \pi_{a,b,c,d}, \quad (29)$$

which refers to the fraction of the collective capacity that has been used by all UEs in all groups. The average total system throughput is obtained by multiplying (29) by  $H$ .

3) *Collision Probability*: Because the model uses a random access channel for connection requests, it is necessary to compute the collision probability of the system. The collision probability for UEs in group  $x$  is:

$$D^{(x)} = \sum_{a,b,c,d} \sum_{k=0}^{N_x-a} \sum_{j=0}^K \beta_k^{(j)} I_{k-j}^{(1)} \pi_{a,b,c,d} \binom{N_x - \eta}{k} p^k (1-p)^{N_x - \eta - k} w_{x,y}^{(u)}, \quad (30)$$

where  $\eta = \{a, d\}$  for group  $x = \{1, 2\}$ , respectively, and  $\eta = b + c$  for group  $x = 3$ .

#### IV. RESULTS

Since our model incorporates a very large number of parameters, in the interest of clarity and brevity we focus our study on certain scenarios that are the most important in the context of our model. First, we present results that demonstrate the impact of a varying channel quality on the load balancing efficiency. Second, we examine the influence of the random access phase on load balancing efficiency. Lastly, we provide insight on the optimal channel sharing policy between BS 1 and BS 2.

To confirm the correctness of the analytical model, we created a simulation environment for verifying the analytical results. The results in Sections IV-A and IV-B are obtained using both the analytical and simulation approaches to confirm correctness, while those in Section IV-C are obtained using only simulation.

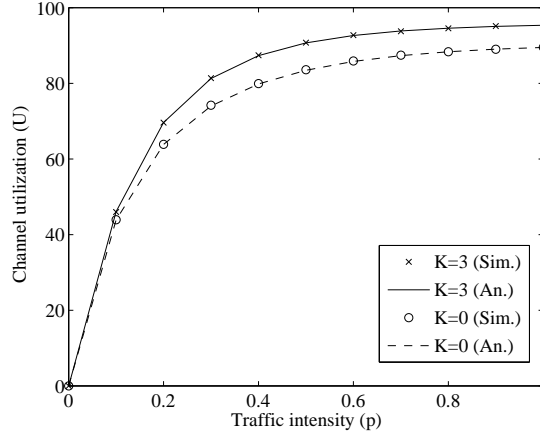


Fig. 2. The channel utilization as a function of traffic intensity  $p$ . Two extremes of shared channels, i.e.  $K = 0$  (no load balancing) and  $K = M_2 = 3$  (all of cell 2's channels used in load balancing) are shown. The figure shows good agreement between the results from the analytical model and from simulation.

#### A. Impact of Channel Quality on Load Balancing Process

In this simulation, we model, among others, the call admission, termination, and load balancing processes exactly as described in our system model. As an example, we consider a scenario in which two identical cells are positioned such that they form a small TTR. For simplicity, we assume that  $N_x = L_x = 6$ , where  $x \in \{1, 2, 3\}$  and  $M_1 = M_2 = K = 3$ . This particular analysis represents the effect of an increasing  $w_{3,1}^{(i)}$  on the overall system-wide channel utilization, while setting  $w_{1,1}^{(i)} = w_{3,2}^{(i)} = w_{2,2}^{(i)} = 0.806$  for all  $i \in \{u, d\}$ , assuming reciprocal uplink and downlink conditions. This is equivalent to varying  $d_{3,1}$  from a location that is out of range to being right next to BS 1, and setting  $d_{1,1} = d_{3,2} = d_{2,2} = 30$  m. We use the pathloss model with the following parameters:  $\gamma_q^{(i)} = -85$  dBm,  $P_t^{(i)} = 30$  dBm,  $W^{(i)} = -31.54$  dB,  $\sigma_\Psi = 3.65$  dB,  $d_{0,x,y}^{(i)} = 1$  m and lastly  $\delta = 4.76$ . Furthermore, we assume an average channel capacity of  $H = 250$  Kbps per channel with an average packet size  $r_p = 1$  kB and  $t_s = 8$  ms slot length. This yields an average packet length of  $1/q = 31.25$  frames, or equivalently 250 ms. The channel throughput represents a typical value used in radio access network planning calculations [27, Table 8.17]. The packet size represents a realistic packet length sent over the Internet [28], where packets are distributed between a minimum value of 40 B (Transport Control Protocol acknowledgement packet) and a Maximum Transmission Unit, which for IPv6 equals 1.268 kB, for IEEE 802.3 equals 1.492 kB, for Ethernet II equals 1.5 kB, and for IEEE 802.11 equals 2.272 kB.

In order to determine the best performance of the load-balancing scheme, represented by the proposed

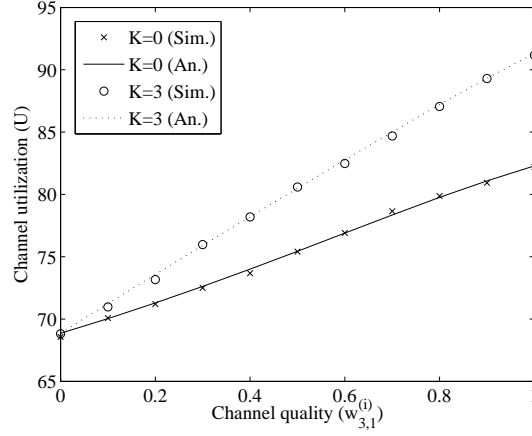


Fig. 3. The channel utilization, represented as a percentage on the vertical axis, as a function of the channel quality between group 3 UEs and BS 1,  $w_{3,1}^{(i)}$  for two extreme values of  $K$ . As  $w_{3,1}^{(i)}$  improves, more group 3 UEs generate successful connections to cell 1 resulting in more UEs that connect to BS 1 and consequently are offloaded onto cell 2, resulting in an overall increase in channel utilization.

$DR_K$  algorithm, for a varying channel quality we determine the level of traffic intensity which results in maximum channel utilization. Fig. 2 expresses the channel utilization as a function of increasing traffic intensity  $p_1 = p_2 = p_3 = p$  for two extreme  $K$  values, i.e.  $K = 0$  (when no load-balancing is used) and  $K = M_2 = 3$  (all of cell 2's channels may be used for load balancing). As expected, the channel utilization increases with more traffic intensity because an increase in  $p$  results in more frequent connection requests from UEs in all groups leading to a higher probability of successful connections. The increase in channel utilization tails off as the system reaches saturation, i.e. close to 100% channel utilization. Similarly, an increase in  $K$  results in a higher channel utilization as more UEs from group 3, that are blocked from cell 1, are offloaded onto cell 2 where they have access to an additional  $K$  channels. We observe that there is a decreasing rate of gain in channel utilization with an increase in the number of shared channels  $K$ . As Fig. 2 shows, a traffic intensity of  $p = 0.4$  results in the most improvement in channel utilization between the two extremes of  $K = 0$ , and  $K = M_2 = 3$ . With the knowledge of decreasing gains in channel utilization with increasing  $K$ , there may exist an intermediate value of  $K$  that not only leads to an improvement in total channel utilization, but also maximizes improvement with respect to the overall UE experience. This value of  $K$  is explored in Section IV-C. In the current section we continue our investigation using  $p = 0.4$  and explore the impacts of channel quality on performance.

Fig. 3 illustrates an increase in channel utilization with an increase in  $w_{3,1}^{(i)}$  for two extreme values of  $K$ . Increasing  $w_{3,1}^{(i)}$  results in group 3 UEs having more successful requests for receiving downlink transmissions because the average channel quality, in which requests are granted for group 3 UEs, improves. Therefore, ignoring the channel effects by assuming perfect channel conditions (also done by setting  $w_{3,1}^{(i)} = 1$  in our model) in the analysis of load-balancing schemes, even for one particular group of UEs, produces a non-trivial difference in the channel utilization and leads to an exaggerated improvement in performance due to load balancing. By selecting a reasonable scheme to determine the channel quality, as presented in Section III-A, we are able to provide a more realistic evaluation of the improvements of load balancing. Note that the average channel utilization significantly increases as more channels can be borrowed from BS 2. When  $w_{3,1}^{(i)}$  increases, the difference in channel utilization between cases  $K = 0$  and  $K = 3$  becomes more profound. This proves that with the low channel quality system-wide improvement from load balancing might not be as significant as in the case of perfect channel conditions.

In Fig. 4 we examine  $B^{(3)}$ ,  $D^{(3)}$ ,  $B^{(1)}$ , and  $B^{(2)}$ , as a function of  $w_{3,1}^{(i)}$  for  $K = \{0, 1, 2, 3\}$ . The scenario used in this result is identical to the one used previously. By comparing an increasing value of  $K$  in Fig. 4(a)–Fig. 4(d) we observe the impact of an increasing number of shared channels on the considered performance benchmarks. The first interesting observation is that irrespective of the value of  $K$  the blocking probability for group 1 UEs,  $B^{(1)}$ , is relatively stable. This means that the quality of service requirements for UEs not involved in load balancing will be met, even with load balancing enabled. Second, as  $K$  increases, blocking probability for group 3 UEs,  $B^{(3)}$ , significantly decreases, which proves the effectiveness of load balancing in this context. Furthermore, the collision probability for UEs in group 3,  $D^{(3)}$ , also reduces because with more shared channels there are fewer unconnected UEs to request connections. Note, however, that the difference in collision probability for an increasing  $K$  is not as significant as observed for the blocking probability. Finally, increasing  $K$  only slightly increases blocking probability  $B^{(2)}$  because these UEs have priority in connecting to any of cell 2's free channels.

Focusing on Fig. 4(d) only, where load balancing is enabled, we note that as  $w_{3,1}$  increases, all curves experience an increase. This can be explained as follows: with an increase in  $w_{3,1}^{(i)}$ , more group 3 UEs are able to generate successful connections to BS 1 resulting in an increase in the contention for sub slots during admission control, and hence an increase in  $D^{(3)}$ . Also, there is an accompanied increase in  $B^{(3)}$  because as more UEs generate successful connections, an increasing number of UEs contend for free channels on both cell 1 (where load balancing does not occur) and cell 2 (where load balancing occurs). Consequently, this also results in an increase in  $B^{(1)}$  and  $B^{(2)}$ . Although these trends are obvious, the

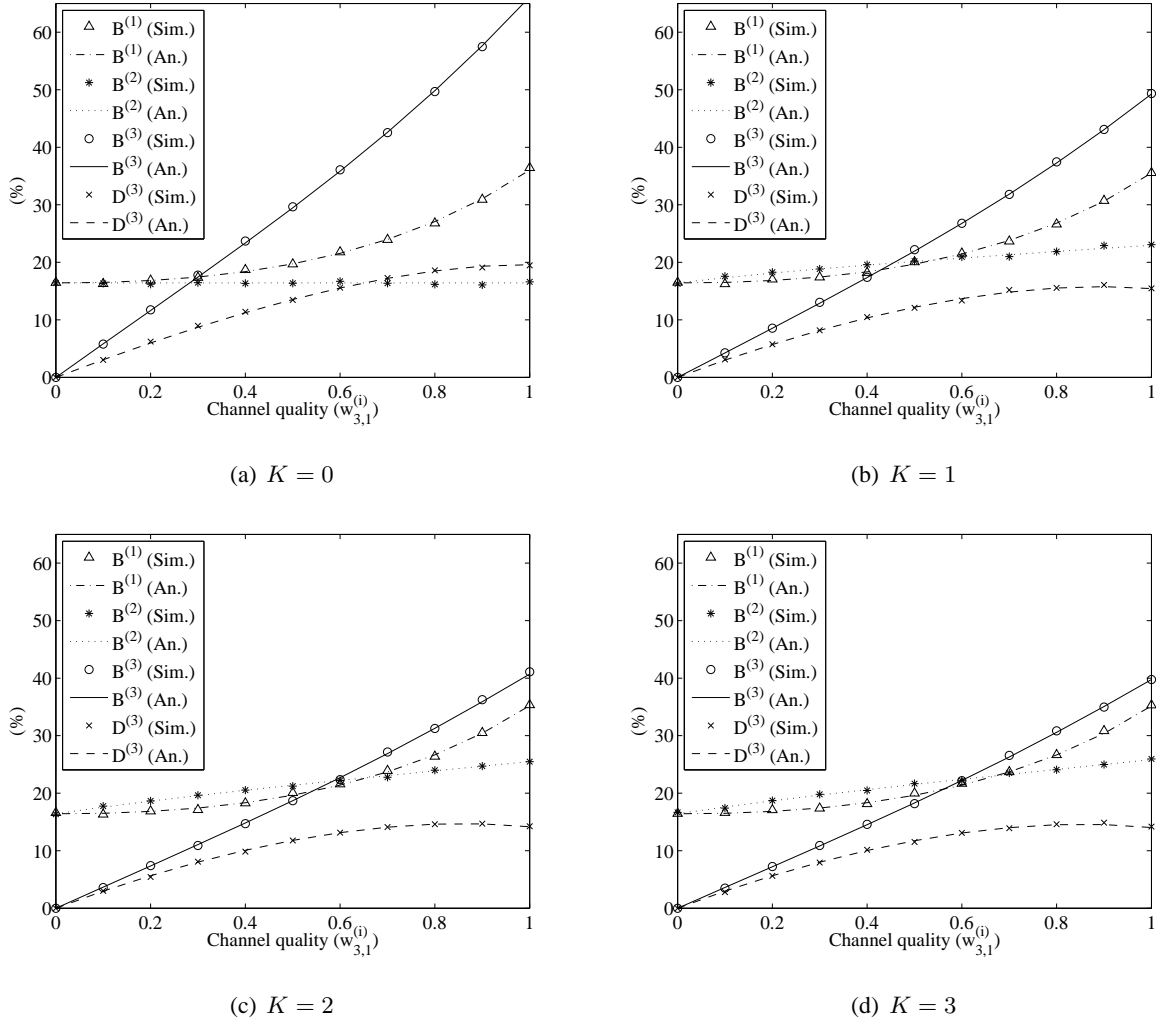


Fig. 4. Illustration of the relationship of the blocking probability for group 3 UEs,  $B^{(3)}$ , the collision probability for group 3 UEs,  $D^{(3)}$ , the blocking probability for group 1 UEs,  $B^{(1)}$ , and the blocking probability for group 2 UEs,  $B^{(2)}$ , as a function of the channel quality between group 3 UEs and BS 1,  $w_{3,1}^{(i)}$  and (a)  $K = 0$ , (b)  $K = 1$ , (c)  $K = 2$ , (d)  $K = 3$ . We observe that the primary factor in the degradation of performance for group 3 UEs in this particular scenario is  $B^{(3)}$  as compared to  $D^{(3)}$  and this difference increases as  $w_{3,1}^{(i)}$  improves. Once again, this figure shows good agreement between the results from the analytical model and from simulation.

exact degradation in UE experience for each group is not. For example, in this specific scenario, Fig. 4 illustrates that  $B^{(3)}$  is always the primary factor in the degradation of the group 3 UE experience as compared to  $D^{(3)}$ . This knowledge is significant as the network operator can determine whether an increase in  $K$ , or an increase  $L_3$  will be more beneficial to group 3 UEs. Observe that Fig. 3 and Fig. 4 show an extremely good match between the analytical result and simulation.

### B. Impact of Random Access Phase on Load Balancing Process

In this section we present results on the effect of random access phase on the performance of load balancing. The results are presented in Fig. 5. All network parameters are set identically to the network considered in Section IV-A, except for  $L_x = 3$ , where  $x \in \{1, 2\}$ .

We begin by investigating the impact of different UE distributions on the performance of load balancing. We perform three experiments and denote each experiment as a specific case. In the first case we set the number of UEs, such that more UEs are distributed in groups 1 and 2, than in group 3, i.e.  $N_1 = N_2 = 6$ ,  $N_3 = 4$ . In the second case we set the number of UEs equal in each group, i.e.  $N_1 = N_2 = N_3 = 6$ . And finally, in the third case we set the number of UEs in group 3 larger than in the other two groups, i.e.  $N_1 = N_2 = 6$ ,  $N_3 = 8$ . The metric that is studied in the three cases described above is the total network-wide blocking probability, calculated as  $\frac{1}{3} \sum_{i=1}^3 B^{(i)}$ , as a function of channel access probability  $p_i = p$  for  $i \in \{1, 2, 3\}$ . This metric is used in order to give a simple overall indication of the blocking suffered by UEs in all groups. Results are presented in Fig. 5(a).

The most interesting observation from Fig. 5(a) is that with an increase in the number of UEs in the TTR, the total blocking probability becomes smaller for moderate values of  $p$ . Surprisingly, the blocking probability starts to drop sharply as the value of  $p$  continues to increase. This phenomenon occurs because as  $p$  increases, so do collisions on the random access channel, which in-turn limits the blocking probability because there are fewer UEs that successfully access available channels. It has to be kept in mind that for each case presented in Fig. 5(a) the length of the random access phase remains the same. What is important to note is that for moderate values of  $p$ , the difference between blocking probabilities for each case is small, i.e. less than 5% (please compare values of blocking probability for each case in the range of  $p \in (0, 0.6)$ ). However, as  $p$  becomes very large, the curves with a higher number of group 3 UEs drop off faster because they experience a substantial increase in the number of collisions. Therefore, a certain value of  $p$  can maximize the channel utilization achieved through load balancing and also maintain the blocking probability at approximately the same level (given negligible changes in UE distribution).

We now move our focus to the impact of random access phase length  $L_x$  on the performance of load balancing. The results are presented in Fig. 5(b). The set of parameters remain the same as in the earlier experiment in this section, however  $p_x = p = 0.4$ . As an example, three network metrics are evaluated as a function of number of slots in the random access phase,  $L_x$ : (i) total channel utilization in both cells,  $U$ , (ii) collision probability at group 3,  $D^{(3)}$ , and (iii) blocking probability at group 3,  $B^{(3)}$ . For clarity, the number of slots is set equal among each group of UEs.

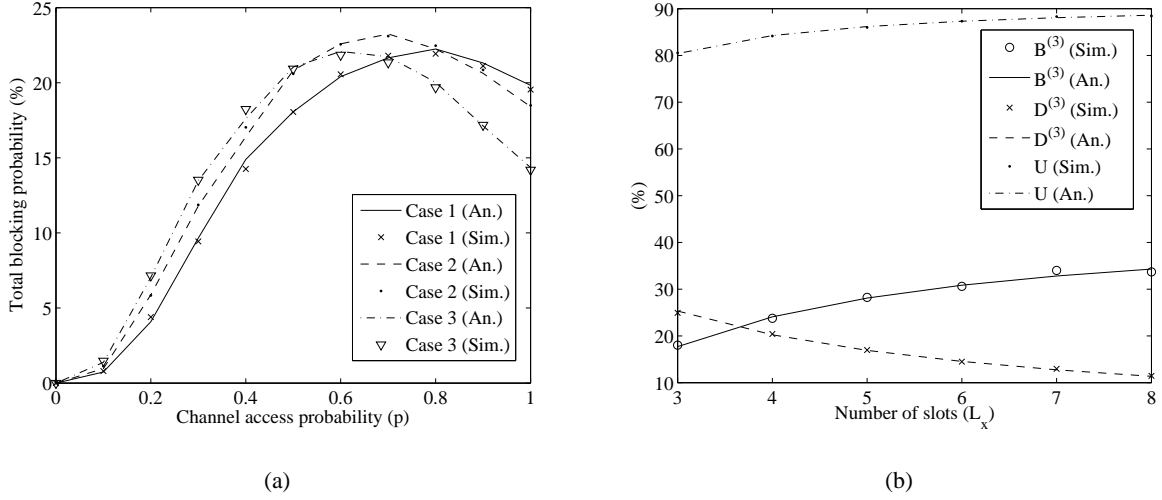


Fig. 5. Impact of random access phase on load balancing process: (a) total network-wide blocking probability as a function of access probability  $p$ ; (b) impact of random access phase length  $L_x$  on the performance metrics of the considered system. We observe that the blocking probability is not a monotonous function of  $p$  and there is an extremum beyond which blocking starts to drop-off. As a result, the network metrics can be easily adapted by the network operator by dynamically selecting number of random access slots.

Obviously, as the number of random access slots increase the collision probability decreases for group 3 UEs, and the overall channel utilization increases. However, as the collision probability decreases the blocking probability, within the same group of UEs, becomes larger. This is in line with the results presented in Fig. 5(a). Recall, that as more UEs gain access to the BS, the probability that channels become unavailable increases. The results shown in Fig. 5(b) further demonstrate the fundamental tradeoff between the delay caused by random access and overall network utilization. Apart from this tradeoff, we demonstrate that the network operator has a powerful tool, i.e. random access phase length, through which network metrics can be easily regulated. It is obvious that the operator has no control over the channel access probability,  $p$ , of individual UEs. However, the operator is able to set a higher value of  $L_x$  to the ASC of interest in order to maintain an expected access delay for each UE against a required blocking probability.

### C. Impact of Varying Shared Channel Pool $K$ on Load balancing Efficiency of $DR_K$

We consider a macrocell scenario in which the distribution of UEs in groups 1, 2 and 3 follow the relationship given by  $N_1 = N_2 < N_3$  and  $L_x = N_x$ , where  $x \in \{1, 2, 3\}$ . Let  $N_1 = N_2 = L_1 = L_2 = 25$  and  $N_3 = L_3 = 40$ . We consider a symmetric system where each cell has 10 channels, i.e.



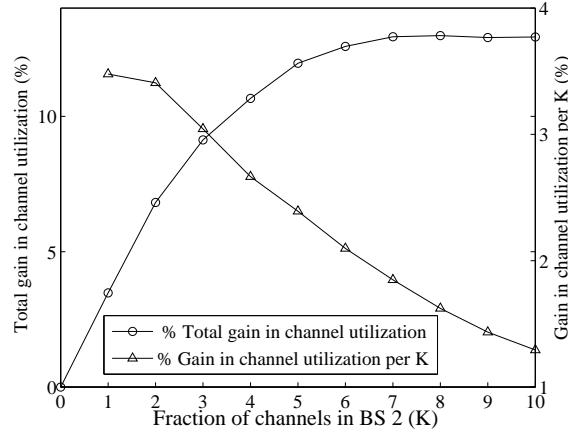


Fig. 6. The percentage improvement of channel utilization (left vertical axis) and the percentage improvement of channel utilization per shared channel (right vertical axis) as a function of shared channels,  $K$ . As  $K$  increases, there is an obvious improvement in channel utilization, however, there are decreasing gains experienced per additional  $K$ .

$M_1 = M_2 = 10$ , and the distances between each group of UEs and their respective serving BSs are identical, i.e.  $d_{1,1} = d_{3,1} = d_{3,2} = d_{2,2} = 220$  m. Once again, we assume an average channel capacity of  $H = 250$  Kbps per channel with an average packet size  $r_p = 1$  kB. A frame duration duration of  $t_s = 1$  ms is used. We assume a simplified path loss model with identical parameters as in Section IV-A except with  $\delta = 3$ , which is more appropriate for outdoor channel conditions.

In Fig. 6 we explore the system-wide improvement in channel utilization (represented as a percentage on the vertical axis) as a function of the number of shared channels  $K$  (represented on the horizontal axis). Note that for the remainder of our study we fix traffic intensity for all groups to  $p = 0.2$  in order to determine the maximum gain in channel utilization for every value of  $K$ . The line with circle markers represents the total percentage improvement experienced as a function of  $K$ , while the line with triangle markers represents the improvement experienced in channel utilization per shared channel. As  $K$  increases, there is a decreasing improvement in channel utilization per additional channel, which indicates that the extra cost of sharing more channels for load balancing may outweigh the added benefit of serving a greater number of UEs.

Although there is an overall improvement in the system-wide channel utilization, the exact effect of the load-balancing scheme on the UE experience is unknown. Obviously,  $B^{(3)}$  decreases with an increase in  $K$  because group 3 has access to more channels. In contrast,  $B^{(2)}$  increases because more UEs in group 3 access channels belonging to cell 2, which are of course also accessible to UEs in group 2. Although

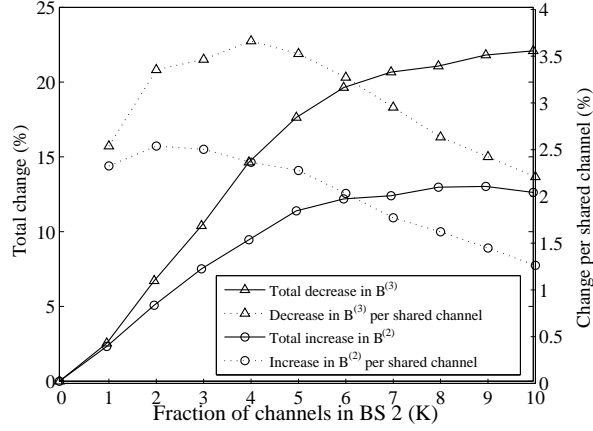


Fig. 7. The total change in blocking probability,  $B^{(x)}$ , and blocking probability per shared channel,  $B^{(x)}/K$ , where  $x \in \{2, 3\}$ . In this scenario, we observe that the decrease in  $B^{(3)}$  is always greater than the corresponding increase in  $B^{(2)}$  for all  $K$ , suggesting that there is an overall improvement in the UE experience. Furthermore, it is seen that at  $K = 6$  we have the greatest difference between the decrease in  $B^{(2)}/K$  and the corresponding increase in  $B^{(2)}/K$  suggesting that this is the optimal number of shared channels to use in order to gain the best UE experience per  $K$ .

these general trends are obvious, the exact relationship between the amount of decrease in  $B^{(3)}$  versus the amount of increase in  $B^{(2)}$  is unknown. In Fig. 7 we examine this relationship in more detail, where the decrease in  $B^{(3)}$  (solid line with triangle markers) is plotted with the consequent increase in  $B^{(2)}$  (solid line with circles) as a percentage on the vertical axis with increasing  $K$  on the horizontal axis. We observe that in this particular scenario the total decrease in  $B^{(3)}$  is always more than the total increase in  $B^{(2)}$ , suggesting that the overall UE experience improves with the proposed load-balancing scheme. This reaffirms the increase in channel utilization with an increase in  $K$  for  $DR_K$ , which is previously observed in Fig. 6.

The total improvement in overall UE blocking probability demonstrates the effectiveness of the load balancing scheme. However, from a network operator viewpoint, knowledge of the changes in UE experience per additional shared channel is also very important. Fig. 7 examines the effect of an increase in  $K$  on both the decrease in  $B^{(3)}/K$  (dashed line with triangles), and the consequent increase in  $B^{(2)}/K$  (dashed line with circles). We observe, that for this particular scenario, a decrease in  $B^{(3)}/K$  is always more than the increase in  $B^{(2)}/K$ , which suggests that the UEs in group 3 experience more of an improvement in performance than the performance degradation experienced by UEs in group 2 per additional shared channel. This allows direct evaluation of the effectiveness of the load-balancing scheme

on the overall UE experience per additional shared channel. In Fig. 7, we note that  $B^{(3)}/K$  reaches a maximum at an intermediate value of  $K$ , i.e.  $K = 3$ , because the system reaches a balance between the number of UEs requesting connections and those that are already connected through load balancing. Our model allows for the direct observation of this system state because of the combined modeling of a finite number of UEs together with a detailed call admission process. With the use of Fig. 7, we are able to determine the best  $K$  to improve the overall UE experience on a per shared channel basis, and then find the corresponding improvement in the overall channel utilization using Fig. 6. For this particular scenario, the maximum difference between the increase in  $B^{(3)}/K$  and decrease in  $B^{(2)}/K$  occurs at  $K = 6$  and corresponds to an overall improvement in channel utilization of 12.6%.

In summary, we can construct the following optimization function. Given fundamental descriptors of the network considered in Section III, i.e.  $N_i$ ,  $M_i$ ,  $L_x$ ,  $p_i$ ,  $w_{x,y}^{(i)}$ ,  $r_p$ , and  $t_s$ , the network operator should find

$$\arg \max_K U/K \text{ subject to } \forall i B^{(i)} \leq b^{(i)}, D^{(i)} \leq d^{(i)}, \quad (31)$$

where  $b_i$  and  $d_i$  are the required maximum blocking and collision probabilities, respectively, for group  $i$ . The developed analytical model provided in Section III allows solving the optimization function (31), since each metric,  $U$ ,  $B^{(i)}$  and  $D^{(i)}$  is given in closed form. The optimization formula allows obtaining the value of  $K$  in order to obtain the maximum utilization per shared channel, such that all considered quality of service metrics required by the operator,  $b_i$  and  $d_i$ , are met. Note that finding the optimal solution to (31) is beyond the scope of this paper.

## V. CONCLUSIONS

We have presented a new analytical model to assess the load balancing process in cellular networks. The model differs in many respects from previous work on load balancing analysis in several important ways. In particular, it incorporates a detailed call admission procedure, addresses traffic prioritization in the connection admission process, and also allows exploration of the impact of channel quality on load balancing efficiency. We have presented a variety of results derived from this framework, and in particular explored the tradeoffs in terms of channel utilization, blocking probability, and collision probability when traffic is transferred from a highly congested cell to a less-loaded neighboring cell.

## REFERENCES

- [1] S. Joshi, P. Pawelczak, J. Villaseñor, S. Addepalli, and D. Čabrić, "Connection admission versus load balancing," in *Proc. IEEE GLOBECOM*, Dec. 6–10, 2010.

- [2] B. Eklundh, "Channel utilization and blocking probability in a cellular mobile telephone system with direct retry," *IEEE Trans. Commun.*, vol. COM-34, no. 4, pp. 329–337, Apr. 1986.
- [3] D. Everitt and D. Manfield, "Performance analysis of cellular mobile communication systems with dynamic channel assignment," *IEEE J. Select. Areas Commun.*, vol. 7, no. 8, pp. 1172–1180, Oct. 1989.
- [4] O. K. Tonguz and E. Yanmaz, "The mathematical theory of dynamic load balancing in cellular networks," *IEEE Trans. Mobile Comput.*, vol. 7, no. 12, pp. 1504–1518, Dec. 2008.
- [5] X. Wu, B. Mukherjee, and D. Ghosal, "Hierarchical architecture in the third-generation cellular network," *IEEE Wireless Commun. Mag.*, vol. 11, no. 3, pp. 62–71, Mar. 2004.
- [6] W. Song, W. Zhuang, and Y. Cheng, "Load balancing for cellular/WLAN integrated networks," *IEEE Network*, vol. 21, no. 1, pp. 27–33, Jan./Feb. 2007.
- [7] E. Yanmaz and O. K. Tonguz, "Dynamic load balancing and sharing performance of integrated wireless networks," *IEEE J. Select. Areas Commun.*, vol. 22, no. 5, pp. 862–872, June 2004.
- [8] J. Laiho, A. Wacker, and T. Novosad, Eds., *Radio Network Planning and Optimisation for UMTS*. Hoboken, NJ, USA: John Wiley & Sons, 2006.
- [9] W. Cooper, J. R. Zeidler, and S. McLaughlin, "Performance analysis of slotted random access channels for W-CDMA systems in nakagami fading channels," *IEEE Trans. Veh. Technol.*, vol. 51, no. 3, pp. 411–424, May 2002.
- [10] Y. Yang and T.-S. P. Yum, "Analysis of power ramping scheme for UTRA-FDD random access channel," *IEEE Trans. Wireless Commun.*, vol. 4, no. 6, pp. 2688–2693, Nov. 2005.
- [11] C.-L. Lin, "Investigation of 3rd generation mobile communication RACH transmission," in *Proc. IEEE VTC-Fall*, Boston, MA, USA, Sept. 24–28, 2000.
- [12] J. He, Z. Tang, D. Kaleshi, and A. Munro, "Simple analytical model for the random access channel in WCDMA," *Electronics Letters*, vol. 43, no. 19, pp. 1034–1036, Sept. 2007.
- [13] H. Jiang and S. S. Rappaport, "Prioritized channel borrowing without locking: A channel sharing strategy for cellular communications," *IEEE/ACM Trans. Networking*, vol. 4, no. 2, pp. 163–172, Apr. 1996.
- [14] W. S. Jeon and D. G. Jeong, "Comparison of time slot allocation strategies for CDMA/TDD system," *IEEE J. Select. Areas Commun.*, vol. 18, no. 7, pp. 1271–1278, July 2000.
- [15] D. Z. Deniz and N. O. Mohamed, "Performance of CAC strategies for multimedia traffic in wireless networks," *IEEE Trans. Wireless Commun.*, vol. 21, no. 10, pp. 1557–1565, Dec. 2003.
- [16] H. Wu, C. Qiao, S. De, and O. Tonguz, "Integrated cellular and ad hoc relaying systems: iCAR," *IEEE J. Select. Areas Commun.*, vol. 19, no. 10, pp. 2105–2115, Oct. 2001.
- [17] A. Gotsis, D. Komninos, and P. Constantinou, "Dynamic subchannel and slot allocation for OFDMA networks supporting mixed traffic: Upper bound and a heuristic algorithm," *IEEE Commun. Lett.*, vol. 13, no. 8, pp. 576–578, Aug. 2009.
- [18] T.-S. P. Yum and W.-S. Wong, "Hot-spot traffic relief in cellular systems," *IEEE J. Select. Areas Commun.*, vol. 11, no. 6, pp. 934–940, Aug. 1993.
- [19] J.-G. Choi, Y.-J. Choi, and S. Bahk, "Power-based admission control for multiclass calls in QoS-sensitive CDMA networks," *IEEE Trans. Wireless Commun.*, vol. 6, no. 2, pp. 468–472, Feb. 2007.
- [20] F. A. Cruz-Peréz, J. L. Vázquez-Ávila, G. Hernández-Valdez, and L. Ortigoza-Guerrero, "Link quality-aware call admission strategy for mobile cellular networks with link adaptation," *IEEE Trans. Wireless Commun.*, vol. 5, no. 9, pp. 2413–2425, Sept. 2006.
- [21] W. Li, H. ang Chen, and D. P. Agrawal, "Performance analysis of handoff schemes with preemptive and nonpreemptive

- channel borrowing in integrated wireless cellular networks,” *IEEE Trans. Wireless Commun.*, vol. 4, no. 3, pp. 1222–1233, May 2005.
- [22] W. Song and W. Zhuang, “Multi-service load sharing for resource management in the cellular/WLAN integrated network,” *IEEE Trans. Wireless Commun.*, vol. 8, no. 2, pp. 725–735, Feb. 2009.
  - [23] S.-P. Chung and J.-C. Lee, “Performance analysis and overflowed traffic characterization in multiservice hierarchical wireless networks,” *IEEE Trans. Wireless Commun.*, vol. 4, no. 3, pp. 904–918, May 2005.
  - [24] D. Choi, P. Monajemi, S. Kang, and J. Villaseñor, “Dealing with loud neighbors: The benefits and tradeoffs of adaptive femtocell access,” in *Proc. IEEE GLOBECOM*, New Orleans, LA, USA, Nov. 30 – Dec. 4, 2008.
  - [25] A. Goldsmith, *Wireless Communications*. New York, NY, USA: Cambridge University Press, 2005.
  - [26] P. Zhou, H. Hu, H. Wang, and H.-H. Chen, “An efficient random access scheme for OFDMA systems with implicit message transmission,” *IEEE Trans. Wireless Commun.*, vol. 7, no. 7, pp. 2790–2797, July 2008.
  - [27] H. Holma and A. Toskala, Eds., *WCDMA for UMTS—HSPA Evolution and LTE*. Hoboken, NJ, USA: John Wiley & Sons, 2010.
  - [28] C. Williamson, “Internet traffic measurement,” *IEEE Internet Comput.*, vol. 5, no. 6, pp. 70–74, Nov./Dec. 2001.